accepted version https://doi.org/10.1002/hyp.15039

Enhancing Runoff Simulation Precision in the Critical Zone through Spatiotemporal Interpolation of Areal Rainfall with Matrix Decomposition

Sheng Sheng[1], Hua Chen[1*], Kangling Lin[1], Yanlai Zhou[1], Jinxing Wang[2], Jie Chen[1], Lihua Xiong[1], Shenglian Guo[1] and Chong-Yu Xu[3]

[1] State Key Laboratory of Water Resources Engineering and Management, Wuhan University, Wuhan, China

[2] Information Center, Ministry of Water Resources, Beijing, China

[3] Department of Geosciences, University of Oslo, Oslo, Norway.

Corresponding Author: Hua Chen, State Key Laboratory of Water Resources and Hydropower Engineering Science, Wuhan University, Wuhan, China

Email: chua@whu.edu.cn

Abstract

Modeling hydrological process in the critical zone not only contributes to a better understanding of interactions across different Earth surface spheres but also holds significant practical implications for water resource management and disaster prevention. Rainfall-runoff simulation in critical zones is particularly challenging due to the amalgamation of temporal and spatial complexity, rainfall variability, and data limitations. As a pivotal input variable of hydrological models, accurate estimation of areal rainfall is critical to successful runoff simulation. However, most estimation methods ignore temporal information, thereby increasing uncertainty in rainfall estimation and constraining the precision of rainfall-runoff simulation. In this study, the matrix decomposition-based estimation method (F-SVD), which considers the spatial and temporal correlation of the rainfall process is employed to estimate areal rainfall. The superiority of the method in producing two-dimensional rainfall information is evaluated through its application in runoff simulation with the Xin'anjiang model. The simulation results of selected flood events in the Jianxi basin in southeast China, spanning from 2009 to 2019, are compared with those of two widely used rainfall estimation methods, namely Arithmetical Mean (AM) and Thiessen Polygons (TP). The results show that (1) F-SVD not only produces the highest Pearson correlation coefficient between rainfall and runoff series but also reduces the number of flood events with abnormal rainfall-runoff relationships; (2) the Xin'anjiang model based on F-SVD achieves the highest Nash-Sutcliffe efficiency and lowest Relative Error, and performs best in simulating peak flow and its occurrence time as compared to AM and TP. This study contributes to a finer characterization of watershed rainfall distribution, enhancing the accuracy and sharpness of runoff simulation. It provides reliable data support for critical zone research and offers a scientific foundation for rationally allocating and managing water resources.

Keywords: areal rainfall estimation, rainfall-runoff simulation, F-SVD, spatiotemporal interpolation, rainfall-runoff correlation, Jianxi basin

1. INTRODUCTION

The critical zone (CZ) is a pivotal region where interactions between the Earth's biosphere, atmosphere, and lithosphere converge (Flinchum et al., 2018). Through comprehensive observations and simulations of diverse ecological, geological, and climatic processes within the CZ, a deeper understanding of the evolution, alterations, and intricate interconnections of surface ecosystems can be unveiled (Brooks et al., 2015). Delving into the hydrological processes within the CZ, coupled with unraveling the embedded rainfall-runoff relationships, precise calculations of rainfall distribution, and meticulous runoff simulations, can furnish a robust scientific foundation for the management of water resources, accurate flood predictions, and effective mitigation strategies against drought.

The CZ often exhibits complex topographical and geomorphological features, leading to the spatiotemporal complexity of rainfall distribution patterns. This necessitates higher-precision models and data to accurately capture these variations. At present, rainfall information is mainly obtained through the following three ways: ground-based rain gauges, radars, and satellites (Wang et al., 2021). These three observation methods' results significantly differ in time and space. Among them, radar and satellite are indirect observation methods. Radar has a high spatial and temporal resolution, but its coverage area is limited, and its accuracy is influenced by the surrounding environment (Wehbe et al., 2020). Meteorological satellites can continuously and quickly provide large-area rainfall information, but it is inferior to radar in spatial and temporal resolution. In addition, there is only an indirect physical relationship between satellite infrared images and rainfall amounts, leading to increased observational errors. The network of rain gauges is the most direct, effective, and common way to observe and collect rainfall data, and its main features are convenient, real-time, and accurate (Michelon et al., 2021; Sreeparvathy & Srinivas, 2022). Thus, it has become the primary data source for rainfall observation. However, since the gauges are distributed irregularly and discretely, they only provide single-point observations, which cannot fully reflect the continuous distribution of spatial rainfall (Cazzaniga et al., 2022). Therefore, using interpolation methods is a fundamental aspect of CZ research, as the precision of rainfall distribution data directly impacts the reliability and effectiveness of these studies.

As a pivotal and active physical process in the hydrological cycle, rainfall is a crucial driver of hydrological processes (Niu et al., 2021; Qiu et al., 2021). The influence of rainfall's temporal and spatial distribution on the hydrological response has long been a hot issue in hydrology (Tao et al., 2021; H. Xu et al., 2013; Y. Zhao et al., 2022). Sapriza-Azuri et al. (2015) investigated the impacts of rainfall spatial variability on the simulated hydrogeological response. They found that the quickly responding soil moisture and actual evapotranspiration fields are largely insensitive to the degree of rainfall spatial variability. In contrast, the slowly responding processes, such as groundwater recharge and the spatial runoff generation processes, are sensitive to local rainfall. Kim and Kim (2020) studied the effect of rainfall spatial distribution on runoff prediction accuracy and found that rainfall spatial distributions affect the relationship between the lower limit of rainfall spatiotemporal resolution for runoff models and runoff prediction accuracy. By providing a reliable foundation, precise runoff simulations pave the way for a more comprehensive comprehension of the dynamic processes occurring within CZ. Consequently, it is imperative to incorporate high-quality rainfall data into runoff simulations to achieve a more accurate representation of runoff processes.

Rainfall estimation methods are chosen for different hydrological models according to the model features and computational efficiency. Lumped hydrological models prefer Arithmetic Mean (AM) (Abu Romman et al., 2021) and Thiessen Polygon (TP) (Verma et al., 2022) to obtain the areal rainfall. Some distributed hydrological models like VIC (Lilhare et al., 2020) use the inverse distance weighting (IDW) to interpolate station data into grids to calculate areal rainfall, others like SWAT (Pang et al., 2020) use the observed data of the nearest rainfall station to the center of the basin as the areal rainfall. A lot of research work has focused on the influence of input data uncertainty on runoff modeling (J. Chen et al., 2020; Goshime et al., 2019; Li & Xu, 2014). Hwang et al. (2020) investigated the impacts of the catchment area on different spatial interpolation schemes, including the TP, IDW, Multiquadric interpolation, and Kriging. They found that the latter two methods better estimate areal mean rainfall on small basins. Errors in rainfall estimation not only hinder our ability to identify other sources of error but also undermine the reliability of operational applications, posing a significant challenge for hydrological modeling (Hjelmstad et al., 2021; Hsueh et al., 2022). Existing research highlights the crucial impact of areal rainfall accuracy on runoff simulation. However, it is essential to recognize that rainfall is not just about its spatial distribution; it also possesses a critical temporal dimension.

The rainfall spatial estimation methods for hydrological models follow the "First Law of Geography" (Tobler, 2004), which separates time from space. Ignoring this temporal correlation can lead to incomplete representations of the hydrological processes within a watershed. To address this limitation and enhance the accuracy of runoff simulations, it becomes imperative to incorporate the temporal dimension into rainfall estimation when conducting runoff modeling. This holistic consideration of both spatial and temporal aspects of rainfall ensures that the simulations more faithfully mirror real-world hydrological processes, ultimately advancing our ability to manage and predict water resources in CZ effectively.

Some scholars have studied rainfall spatiotemporal interpolation methods (Hussain et al., 2010; Vargas et al., 2021). Militino et al. (2015) proposed two natural and simple extensions to kriging and thin-plate splines to incorporate time dependence into the statistical model. They validated the accuracy and efficiency of predictions from daily observations collected from 87 manual rainfall gauges from 1990 to 2010 in Navarre, Spain. Saha et al. (2020) proposed a spatio-temporal hybrid modeling approach by integrating Space-Time Autoregressive Moving Average (STARMA), artificial neural network, and support vector machine and revealed that the proposed spatio-temporal hybrid approach had better modeling and forecasting precision over conventional STARMA. However, it's worth noting that some of these approaches tend to be relatively complex in terms of practical implementation. In our previous study (H. Chen et al., 2021), the concept of the recommender system, which predicts users' preference for products based on historical interactions, was introduced into rainfall estimation. A matrix decomposition-based rainfall spatiotemporal interpolation method was proposed to incorporate the rainfall temporal information and spatial distribution of rain gauges. Through a cross-validation experiment involving 176 rain gauges in the middle and upper reaches of the Hanjiang River basin, it was verified to have better accuracy and stability than IDW and ordinary kriging (OK). The mentioned interpolation method offers higher portability and ease of use. By applying this method to areal rainfall calculation and runoff simulation, we aim to investigate whether incorporating spatiotemporal information related to the rainfall process in hydrological simulations can accurately represent the physical relationship between rainfall and runoff. This, in turn, has the potential to enhance the precision of runoff simulations within the CZ.

The objectives of this study are threefold: (1) to improve the accuracy of areal rainfall estimation through spatiotemporal interpolation, which can offer more reliable data support for studies conducted within the CZ; (2) to evaluate the impact of the mean areal rainfall on rainfall-runoff relationship and runoff simulation, which considers calculation methods based on spatial relationship and spatiotemporal relationship; and (3) to enhance the accuracy and sharpness of runoff simulation through incorporating spatiotemporal interpolated rainfall, which enables better prediction and management of water resources and flood risks in the CZ. In this study, the matrix decomposition-based interpolation method inspired by Recommender Systems is applied to calculate the areal rainfall considering the spatiotemporal information. Based on the estimated areal rainfall, the rainfall-runoff modeling is conducted through the Xin'anjiang model, and its performance is compared with the model driven by rainfall calculated by Arithmetic Mean and Thiessen Polygon to explore the effect of spatial and temporal rainfall information on runoff simulation.

2. METHODS

The main research steps of this study are shown in Figure 1.

[Insert Figure 1]

2.1 Spatiotemporal rainfall estimation method based on F-SVD

In our previous study (H. Chen et al., 2021), a rainfall spatiotemporal interpolation method based on matrix decomposition (hereafter referred to as F-SVD) was proposed. Cross-validation confirms that compared with traditional interpolation methods (inverse distance weight, ordinary kriging, etc.), F-SVD can reduce the estimation error and offer a better spatial estimation. The calculation process of F-SVD is shown in

Figure 2 and consists of the following steps:

[Insert Figure 2]

a. For the rainfall estimation of the target point at a particular moment, *m* surrounding gauges and *n* adjacent influencing moments containing the previous rainfall information must be determined.

b. The rainfall data of the surrounding gauges and the target point at adjacent moments can form a spatiotemporal rainfall data matrix *R* sized of $(m+1)*n$, where the rows and columns represent the relationship between time and space, respectively.

c. For the historical rainfall of the target point in the matrix, if there are unknown null values, the traditional interpolation method should calculate the corresponding rainfall until only one element in the matrix representing the rainfall to be estimated is a null value.

d. The F-SVD method decomposes the spatiotemporal rainfall data matrix into a temporal feature matrix *X* and a spatial feature matrix *Y* (as shown in Figure 3), and the stochastic gradient descent algorithm is used for optimization.

e. The two optimal feature matrices are then multiplied to obtain the reconstruction matrix *P*, the element of $m+1$ row and *n* column in the reconstructed matrix is the estimated rainfall, which is calculated as follows:

$$P_{\mathrm{i,j}} = \sum_{q=1}^{q} X_{\mathrm{i,q}} Y_{\mathrm{q,j}} \tag{1}$$

where *q* is the number of latent features.

[Insert Figure 3]

In this study, the study area is divided into 0.1°×0.1° grids, and the proposed spatiotemporal interpolation method based on matrix decomposition is combined with IDW to calculate the rainfall of each grid point, and the areal rainfall is spatiotemporally estimated as the result of arithmetic mean values of all grid points.

2.2 Xin'anjiang model

The Xin'anjiang model is a conceptual rainfall-runoff model proposed by Zhao (1992), which has gained significant popularity and recognition in hydrology, particularly in China (Qi et al., 2022; W. Yang et al., 2020). It has been widely utilized in numerous studies conducted in humid and semi-humid areas (Qi et al., 2021; Wan et al., 2021; X. Yang et al., 2020), demonstrating the model's effectiveness and practical applicability in simulating rainfall-runoff processes. The Xin'anjiang model consists of evapotranspiration, runoff production, runoff separation, and flow routing modules. The evapotranspiration module uses a three-layer evapotranspiration model that divides the soil into three layers and calculates the actual evapotranspiration based on the soil water content and potential evapotranspiration. The runoff production module is based on the basin storage capacity curve, which considers the spatial heterogeneity of soil water storage. The runoff separation module divides the total runoff into three water sources: surface runoff, interflow, and groundwater, concerning the theory of hillside hydrology using a free water storage reservoir. In the flow routing module, considering the differences in the flow confluence processes of the three water sources, the surface runoff is confluent by the unit line method, and interflow and groundwater are confluent by linear reservoirs.

The calculation of these four modules of the Xin'anjiang model involves 15 parameters shown in Table 1, which can be calibrated by the Shuffled Complex Evolution method developed at The University of Arizona (SCE-UA) (Duan et al., 1994). This study uses the spatiotemporally estimated rainfall in step 1 as the areal rainfall to drive the Xin'anjiang model for runoff simulation. Two commonly used areal rainfall calculation methods, namely the AM and TP, are used to obtain the areal rainfall for comparison. When calibrating parameters using optimization algorithms, there is inherent uncertainty. To mitigate the potential impact of this uncertainty on runoff simulation results, we employed the same set of parameters when comparing the simulation outcomes of the Xin'anjiang model using three different areal rainfall datasets. Specifically, we used the optimal parameters derived from the calculated mean areal rainfall series by AM.

[Insert Table 1]

2.3 Model evaluation indicators

A cross-validation method is used to validate the proposed rainfall estimation method. Using the leave-one-out method, the F-SVD method is combined with IDW to interpolate the rainfall at each gauge. Four indicators are selected to evaluate the accuracy, namely root-mean-square error (*RMSE*), mean average error (*MAE*), percentage error (*PERC*), and two-sample Kolmogorov-Smirnov test statistic (*KS*). *RSME* and *MAE* represent the absolute deviation between estimation and observation, *PERC* represents the relative error, and *KS* checks whether the distributions of the two data are consistent. The low values of those indicators suggest a high accuracy of the estimation method. The computations of *RMSE*, *MAE*, *PERC,* and *KS* values are described below.

$$RSME = \sqrt{\frac{1}{n}\sum_{i=1}^{n}(z_i^{sim} - z_i^{obs})^2} \tag{2}$$

$$MAE = \frac{1}{n}\sum_{i=1}^{n}\left|z_i^{sim} - z_i^{obs}\right| \tag{3}$$

$$PERC = \frac{1}{n_1 + n_2}\left(\sum_{i=1}^{n_1}\left|\frac{z_i^{sim} - z_i^{obs}}{z_i^{obs}}\right| + n_2\right) \tag{4}$$

$$\begin{cases} \sup\limits_{x\in R}\left|F_1(x) - F_2(x)\right| \le d_p, KS_i = 0 \\ \sup\limits_{x\in R}\left|F_1(x) - F_2(x)\right| > d_p, KS_i = 1 \\ KS = \frac{1}{n}\sum_{i=1}^{n} KS_i \end{cases} \tag{5}$$

where z_i^{obs} and z_i^{sim} are the observed and estimated rainfall at the *i*-th gauge; n_1 is the number of moments when the rainfall is not zero; n_2 is the number of rainless moments estimated to be rainy; F_1 and F_2 indicate the distribution functions of estimation and observation series of the i-th gauge; d_p denotes the critical value at the significance level $p = 5\%$.

To evaluate the effect of considering the spatial and temporal relationship of rainfall on the runoff simulation, the areal rainfall estimation by the proposed method is input into the hydrological model for validation. The elements describing floods include flood hydrograph, flood volume, peak flow, and peak occurrence time. To comprehensively evaluate the simulation results, besides two commonly used indicators, including the Nash-Sutcliffe efficiency coefficient (*NSE*) and the relative error of water balance (*RE*), two other indicators, namely the peak occurrence time difference (*tAE*) and the relative error of flood peak flow (*vRE*), are also selected to evaluate the effect of spatiotemporal estimated rainfall on the simulation of flood peak. *NSE* indicates the degree of agreement between the simulated flood hydrograph and the observed one; the closer the value is to 1, the better the runoff simulation. *RE* reflects the accuracy of the total flood volume; the closer the value is to 0, the better the simulation result. *tAE* refers to the difference between when the maximum flood flow occurs in the simulated and actual floods. *vRE* reflects the simulation error of peak flow, i.e., the maximum flow in the flood process; the smaller the value, the better the peak flow simulation. The calculation equations are as follows:

$$NSE = 1 - \frac{\sum_{i=1}^{n}\left[y_c(i) - y_0(i)\right]^2}{\sum_{i=1}^{n}\left[y_0(i) - \overline{y_0}\right]^2} \qquad (6)$$

$$RE = \left|\frac{\sum_{i=1}^{n} y_c(i) - y_0(i)}{\sum_{i=1}^{n} y_0(i)}\right| \qquad (7)$$

$$tAE = Time_c\,|_{y_c=\max(y_c)} - Time_0\,|_{y_0=\max(y_0)} \qquad (8)$$

$$vRE = 100 \times \frac{\max(y_c) - \max(y_0)}{\max(y_0)}\% \qquad (9)$$

where y_c and y_o represent the simulated and observed runoff process of floods; $Time_c$

and $Time_o$ are the peak occurrence time of simulated and observed floods.

3. STUDY REGION & DATA

The Jainxi basin is located in southeast China. The topography of the watershed is diverse, characterized by multi-sided surrounding mountains, resulting in intricate terrain and the formation of a complex river network. The basin experiences a subtropical monsoon climate with warm and humid weather. Seasonal rainfall patterns are evident, with April to June being the plum rain season and July to September being the typhoon rain season. The vegetation within the basin is varied, with extensive coverage of mountain forests, accounting for 78.75% of the land area. Additionally, 15.81% of the area is farmland, while grasslands cover 3.95%. Influenced by natural factors such as terrain, climate, and vegetation, as well as human factors, including land use types, most of the basin is prone to soil erosion and is highly sensitive to human activities due to its delicate ecosystem. Some areas are characterized by geological structures and materials susceptible to landslide events. Coupled with frequent heavy rainfall, this contributes to the occurrence of geological hazards. The hilly and mountainous terrain and swift water flow make the watershed susceptible to rapid runoff during heavy rain, increasing the risk of flooding. Overall, the Jianxi basin exhibits diverse landforms, varied geological conditions, rich soil and vegetation, and a complex ecological environment.

Accurate flood simulation is of paramount importance for enhancing disaster risk management capabilities and preserving the ecological environment in this basin. Understanding the rainfall-runoff relationship is crucial for the region's water resource management and flood control efforts. Previous research conducted in the Jianxi basin has explored the evolution of rainfall and runoff processes (Cui et al., 2022; Jie et al., 2018; Li et al., 2022; Sheng et al., 2020), yet these analyses primarily relied on rainfall spatial distribution information, neglecting the effect of temporal dynamics on rainfall estimation. This study aims to enhance our understanding of the role of two-dimensional spatial and temporal rainfall information in improving the accuracy and sharpness of runoff simulation.

The spatial distribution of hydrological stations and sub-basins is shown in Figure 4. The whole basin has 7 hydrological stations, 15 rainfall stations, and 3 evaporation stations. Hourly hydrological data of 45 flood events from 2000 to 2019 are selected as the research data in this study.

[Insert Figure 4]

4. RESULTS

4.1 Evaluation of interpolation accuracy on rainfall events

According to the flow process of the 45 flood events, the corresponding rainfall events are selected, and the rainfall of each gauge is estimated by the leave-one-out method. The estimation accuracy of each gauge is evaluated using four indicators, and the results are presented in Figure 5 as a box plot. From the figure, it can be seen that F-SVD outperforms the IDW method in terms of all indicators. Compared with IDW, F-SVD has a lower mean value and less uncertainty, indicating a higher precision and proving that considering spatial and temporal information for rainfall estimation is helpful for accuracy improvement.

[Insert Figure 5]

To further evaluate the performance of the interpolation method in the cross-validation, two typical rain events, including a heavy rain event (June 17 to June 28, 2005) and a light rain event (May 25 to May 30, 2016), are selected for comparative analysis, and the results are shown in Figure 6. The four subgraphs show, in order, the accumulated rainfall, the errors of the IDW and F-SVD evaluated by *RSME*, and the improvement rate of the estimation accuracy achieved by F-SVD. From the results of gauges' estimation errors in Figure 6(b) and Figure 6(c), it is clear that gauges with large rainfall values tend to produce large estimation errors as well. In Figure 6(d), there are few blue dots with an improvement rate of less than 0, which means the accuracies of most gauges are improved using the F-SVD method. Besides, the number of gauges with higher accuracy is larger for the heavy rain event than for the light rain event. As for the few points with small cumulative rainfall or uneven distribution of surrounding gauges, the information in the spatiotemporal rainfall matrix is not comprehensive and integrated enough to be effectively decomposed and reconstructed, resulting in no improvement in accuracy. The superiority of F-SVD in the Jianxi basin in this study is consistent with the findings of our previous study, which demonstrated the advantage of F-SVD over IDW and OK in the cross-validation of 176 rain gauges in the Hanjiang River basin (H. Chen et al., 2021). Therefore, the F-SVD method can effectively extract spatial and temporal features from the historical precipitation, improving the accuracy of interpolation, particularly in basins with abundant rainfall.

[Insert Figure 6]

4.2 Correlation analysis of rainfall and runoff

The Jianxi watershed is divided into several sub-basins according to the spatial distribution of runoff stations, and the proposed spatiotemporal interpolation method F-SVD is used to calculate the mean areal rainfall of each sub-basin, which is compared with the other two widely used calculation methods, including AM (Arithmetical Mean) and TP (Thiessen Polygons). The Pearson correlation coefficients between the three mean areal rainfall series and runoff observation series are calculated for each sub-basin, and the correlation coefficient matrices are averaged and drawn into a heat map shown in Figure 7. As a statistical measure that quantifies the strength and direction of the relationship between two variables without considering the absolute differences in their values, the Pearson correlation coefficient ranges between -1 and +1, where +1 represents a perfect positive correlation. It can be seen from the figure that there is a strong correlation between the mean areal rainfall calculated by AM and TP with the Pearson correlation coefficient above 0.9, meaning that as one variable increases, the other variable tends to increase as well. In contrast, F-SVD differs from those two methods in variation since the correlation is slightly lower. Besides, the runoff series demonstrates the highest correlation with the mean areal rainfall series computed using

F-SVD, while the correlations between the other two mean areal rainfall series and runoff are very similar, with TP exhibiting a slightly higher correlation.

[Insert Figure 7]

For each sub-basin, the relationship between the cumulative rainfall and runoff depth is analyzed by estimating the determination coefficient using linear regression (Tirkey et al., 2014), and the result is shown in Figure 8, where red dots indicate the abnormal floods when runoff depth exceeds total rainfall. It can be seen from the figure that the determination coefficient is above 0.9 in different sub-basins, a typical phenomenon in humid regions, indicating that strong correlations exist between runoff depth and cumulative rainfall calculated by the three methods (Gupta & Dixit, 2022). Meanwhile, when F-SVD is used to calculate the cumulative rainfall, the rainfall-runoff determination coefficient (R^2) of the floods is the highest, and the abnormal situations where the total rainfall is less than the runoff decrease. Although F-SVD may exhibit greater accuracy at the hourly scale, these effects tend to average over time, reducing the noticeable differences in cumulative rainfall. Calculating cumulative rainfall can involve statistical offsetting of the data, resulting in a relatively small improvement in R^2 and linear regression slopes. In summary, F-SVD provides areal rainfall series with a higher correlation with runoff series, and the good relationship between rainfall and runoff is essential to successful rainfall-runoff modeling and accurate runoff forecasting (Saft et al., 2015).

[Insert Figure 8]

4.3 Evaluation of runoff simulation based on different areal rainfall

According to the calculated mean areal rainfall series, the parameters of the Xin'anjiang model are calibrated using the SCE-UA algorithm. To avoid the influence of the uncertainty in the optimal parameters on the simulation results, three different rainfall data are input to the Xin'anjiang model for runoff simulation using the same set of parameters calibrated by AM (Table 2), and the comparison results are shown in Table 3. At the same time, the simulation results of the calibrated parameters based on TP and

F-SVD are also attached to the table. For each sub-basin, the Xin'anjiang model driven by the rainfall of F-SVD achieves the highest NSE, lowest RE, tAE, and vRE in almost all cases. Compared with AM and TP, F-SVD increases the value of *NSE* by 7.5% and 5.7% and decreases the value of *RE* by 58.8% and 56.5%, respectively. The improvement rate of *tAE* reaches 16.9% and 8.8%, and that of *vRE* reaches 10.7% and 9.27%, respectively. The evaluation results of different indicators are consistent; that is, the accuracy of runoff simulation based on F-SVD is the highest, followed by TP, and that of AM is the lowest. And this difference in accuracy is more obvious in smaller sub-basins. The difference between the simulation results of three rainfall data using the same set of parameters is similar to that using its own calibrated parameters, and the accuracy is slightly higher using their own calibrated parameters.

[Insert Table 2]

[Insert Table 3]

The evaluation accuracy of all selected flood simulation results using different mean areal rainfall in each sub-basin is shown in Figure 9. It can be seen from the figure that, compared with large sub-basins (JY, QLJ), the medians of the boxplot of the three methods are lower, and the intervals are wider in small sub-basins (MS, WYS, SX), indicating that there are more uncertain and more challenging to simulate runoff in small sub-basins. Furthermore, the interval widths and median values of AM and TP simulation results are similar for most watersheds. At the same time, the evaluation results of the runoff simulation using F-SVD to calculate the mean areal rainfall are improved compared with the other two methods in terms of median value and interval width, indicating that using F-SVD to calculate rainfall for runoff simulation has higher accuracy and smaller uncertainty.

[Insert Figure 9]

4.4 Runoff simulation results of typical floods

To better compare the differences in runoff simulation using different mean areal rainfall, three typical flood events, corresponding to P=80%, P=50%, and P=1% floods

(P is the flood frequency of exceedance), are selected to compare the difference between the simulated and the observed flood hydrographs. Based on the river levels observed at the outlet stations of the basin (refer to Figure 4) and the corresponding basin areas (see Table 3), two small sub-basins, MS and SX, and two large sub-basins, JY and QLJ, are chosen to perform the evaluation. The simulation results of typical floods in these selected basins are depicted in Figure 10. It can be found from the figure that, on the whole, the runoff simulation result in large sub-basins is better than that in small sub-basins, which is consistent with other research results (Ghimire et al., 2022; Merz et al., 2009). Floods in small sub-basins have the characteristics of steep rise and fall, rapid peak formation, and complex runoff generation and concentration processes, increasing the difficulty of runoff simulation (Chen et al., 2022). However, whether in small sub-basins or large sub-basins, when using F-SVD to calculate the mean areal rainfall for runoff simulation, the simulated hydrograph fits better with the observed one, and the peak value and peak occurrence time of the simulated flood are also more accurate. Besides, the runoff simulation based on AM has the poorest performance, especially in the simulation of flood peaks. Due to the considerable temporal and spatial variation of rainfall during flood events, the station observation data cannot fully reflect the spatial distribution of rainfall in the basin; thus, it is hard to accurately simulate the runoff by calculating the mean areal rainfall using AM (Gentilucci et al., 2022). For example, in the Qilijie basin, the simulated flood peaks of small and medium floods are earlier than the observed ones.

[Insert Figure 10]

5. DISCUSSION

Rainfall data is characterized as spatiotemporal structured data, exhibiting correlations and continuity in both time and space (Liu et al., 2022). The F-SVD method leverages the rainfall data matrix to uncover latent temporal and spatial features from historical rainfall information, then employs the derived feature matrices to estimate rainfall at the interpolation point. This approach's superior accuracy, demonstrated through cross-validation in the Jianxi basin (Figure 5), outperforms the IDW method. This finding is consistent with our earlier research, where F-SVD's accuracy surpassed traditional methods, including IDW and OK, which rely on spatial relationships for interpolation. Other researchers have also noted the enhanced accuracy from considering temporal correlations in rainfall data during estimation (Cassiraga et al., 2021; Xu et al., 2019). Among rainfall events of different intensities, heavy rainfall displays robust spatiotemporal characteristics and correlations (Li et al., 2022), offering richer and more valuable information (Wu et al., 2020). Consequently, the advantages of F-SVD over traditional interpolation methods are particularly pronounced when dealing with high-intensity rainfall events (Figure 6).

The interpolation of rainfall data using the F-SVD method is extended to cover each grid point within the Jianxi basin, and the resulting values are then aggregated through arithmetic averaging to derive areal rainfall. Compared to commonly employed methods such as AM and TP, the spatiotemporal-interpolated areal rainfall demonstrates a more reasonable and coherent relationship with runoff patterns. This enhanced coherence is particularly evident through the amplified correlation between rainfall and runoff sequences, as depicted in Figure 7. Moreover, adopting the F-SVD method helps alleviate instances where flood runoff depths surpass total rainfall amounts (Figure 8). When applying estimated areal rainfall in runoff simulation, the advantages of utilizing F-SVD-derived areal rainfall become pronounced. By employing different areal rainfall datasets as inputs for the hydrological model parameter optimization through the SCE-UA method, the accuracy during the validation period, as indicated in parentheses in Table 3, reveals that simulations based on F-SVD-derived rainfall consistently outperform those based on TP and AM. The utility of the F-SVD method extends beyond simply improving rainfall-runoff relationships. The implications of its application carry significant potential for enhancing hydrological modeling and predictions across various watersheds.

The uncertainty inherent in the computation of areal rainfall can introduce biases in parameter estimation, subsequently impacting model simulation accuracy (McMillan et al., 2011). In the context of this study, we have temporarily set aside the potential influence of model structure and parameters on simulation outcomes. Instead, we have attributed changes in streamflow simulation results solely to rainfall input variations stemming from different interpolation methods. When conducting a comparative analysis of different areal rainfall simulation outcomes, we maintain consistency by utilizing the same set of parameters, i.e., the rate-optimal parameters for surface rainfall calculated using the AM method (Table 2). Notably, due to the higher precision of F-SVD-derived areal rainfall calculations, the runoff simulation results exhibit enhanced accuracy and greater stability (Table 3, Figure 9). This outcome highlights that the quality of rainfall inputs can significantly influence the outcomes of runoff simulations (Fraga et al., 2019). It is worth noting that the distribution of rainfall directly affects the shape of the flooding process, particularly the peak flow, which often exhibits a close correlation with short-duration high-intensity rainfall events (Kabir et al., 2022). F-SVD, with its superior accuracy and sensitivity to temporal correlations, particularly shines under conditions of high-intensity rainfall. As such, it delivers more precise peak flow values and accurate peak occurrence times in its runoff simulations (Figure 10). The finding reinforces that accounting for the spatiotemporal characteristics in calculating surface rainfall is essential for achieving reliable and accurate hydrological modeling outcomes.

The spatiotemporal interpolation approach employed in this study presents the potential for seamless expansion to diverse CZ. This adaptability allows for using observed data from rainfall stations to interpolate areal rainfall, consequently producing more accurate estimates than traditional interpolation techniques solely reliant on spatial relationships. This methodology's versatility extends beyond rainfall data. It can be harnessed to interpolate other spatiotemporal structured datasets within hydrology, encompassing temperature, soil moisture, and more variables. Furthermore, the derived areal rainfall distribution can be harnessed to drive distributed hydrological models, including well-established frameworks like the SWAT and the VIC model. By incorporating high-quality areal rainfall data as input, these models can produce more accurate and finely-tuned runoff simulations, thus contributing to the advancement of hydrological simulation and prediction methodologies. In sum, the spatiotemporal interpolation method enhances the accuracy of rainfall estimation and runoff simulation. Its adaptability and potential for integration with established modeling approaches underscore its significance in advancing the accuracy of hydrological process simulation in CZ.

6. CONCLUSIONS

In this study, the spatiotemporal rainfall estimation method based on matrix decomposition is proposed and applied to areal rainfall calculation to improve the accuracy of the estimation. The Xin'anjiang model is built based on the spatiotemporal rainfall information to simulate runoff. Finally, the rainfall estimation and runoff simulation results are compared with two other methods, namely Arithmetical Mean and Thiessen Polygons. The conclusions are as follows:

(1) The F-SVD method performs better in cross-validation than the traditional methods and proves that considering spatial and temporal information for rainfall estimation is helpful for accuracy improvement.

(2) When using the F-SVD method to calculate the areal rainfall spatiotemporally, the Pearson correlation coefficient between the areal rainfall series and the runoff series is the highest, and the rainfall-runoff determination coefficient of flood events reaches 0.97.

(3) The Xin'anjiang model built based on the spatiotemporally estimated rainfall not only achieves the highest *NSE* and lowest *RE*, *tAE*, and *vRE* but also shows smaller uncertainty and better stability in runoff simulation. The improvement of *NSE* and *RE* reaches 7.5% and 5.7%, and 58.8% and 56.5%, respectively, compared with the model based on rainfall estimated by AM and TP.

(4) The F-SVD method comprehensively utilizes the spatial relationship of rainfall stations and the temporal variation of rainfall time series to calculate mean areal rainfall; thus, the simulated flood's peak flow and peak occurrence time are more accurate than traditional areal rainfall calculation methods.

The spatiotemporal interpolation method in this study facilitates a more refined estimation of basin rainfall distribution, which offers more reliable data support for disaster early warning and resource management within the CZ. The improved rainfall interpolation results can further refine the precision of flood simulations, which stands as a cornerstone element of the study of hydrological and ecological processes in the CZ. The accuracy of runoff simulations not only directly influences the reliability and efficacy of other research facets but also underpins their overall credibility and effectiveness.

Though the proposed approach is demonstrated in one study region in southeast China, it is anticipated to be easily used for areal rainfall estimation or rainfall-runoff modeling in other river basins, especially in areas with ample rainfall or dense distribution of rain gauges. The temporal and spatial unevenness of the rainfall process increases the complexity of the hydrological process mechanism and reduces the accuracy of the hydrological simulation; thus, in future research, the temporal and spatial uncertainty of rainfall will be taken into account to improve the relationship between the relative deviation of the mean areal rainfall and runoff simulation.

ACKNOWLEDGEMENTS

This work was supported by the National Key Research and Development Program of China [2021YFC3200303] and the Research Council of Norway [FRINATEK Project 274310].

DATA AVAILABILITY

The data are obtained from the Fujian Hydrology Bureau and are not publicly available due to their privacy policy.

REFERENCES

Abu Romman, Z., Al-Bakri, J., & Al Kuisi, M. (2021). Comparison of methods for filling in gaps in monthly rainfall series in arid regions. *International Journal of Climatology, 41*(15), 6674-6689. doi:https://doi.org/10.1002/joc.7219

Brooks, P. D., Chorover, J., Fan, Y., Godsey, S. E., Maxwell, R. M., McNamara, J. P., & Tague, C. (2015). Hydrological partitioning in the critical zone: Recent advances and opportunities for developing transferable understanding of water cycle dynamics. *Water Resources Research, 51*(9), 6973-6987. doi:https://doi.org/10.1002/2015WR017039

Cassiraga, E., Gómez-Hernández, J. J., Berenguer, M., Sempere-Torres, D., & Rodrigo-Ilarri, J. (2021). Spatiotemporal Precipitation Estimation from Rain Gauges and Meteorological Radar Using Geostatistics. *Mathematical Geosciences, 53*(4), 499-516. doi:10.1007/s11004-020-09882-1

Cazzaniga, G., De Michele, C., D'Amico, M., Deidda, C., Ghezzi, A., & Nebuloni, R. (2022). Hydrological response of a peri-urban catchment exploiting conventional and unconventional rainfall observations: the case study of Lambro Catchment. *Hydrology and Earth System Sciences, 26*(8), 2093-2111. doi:10.5194/hess-26-2093-2022

Chen, H., Sheng, S., Xu, C.-Y., Li, Z., Zhang, W., Wang, S., & Guo, S. (2021). A spatiotemporal estimation method for hourly rainfall based on F-SVD in the recommender system. *Environmental Modelling & Software*, 105148. doi:https://doi.org/10.1016/j.envsoft.2021.105148

Chen, J., Li, Z., Li, L., Wang, J., Qi, W., Xu, C.-Y., & Kim, J.-S. (2020). Evaluation of Multi-Satellite Precipitation Datasets and Their Error Propagation in Hydrological Modeling in a Monsoon-Prone Region. *Remote Sensing, 12*(21). doi:10.3390/rs12213550

Chen, L., Yan, Z., Li, Q., & Xu, Y. (2022). Flash Flood Risk Assessment and Driving Factors: A Case Study of the Yantanxi River Basin, Southeastern China. *International Journal of Disaster Risk Science, 13*(2), 291-304. doi:10.1007/s13753-022-00408-3

Cui, Z., Zhou, Y., Guo, S., Wang, J., & Xu, C.-Y. (2022). Effective improvement of multi-step-ahead flood forecasting accuracy through encoder-decoder with an exogenous input structure. *Journal of Hydrology, 609*, 127764. doi:https://doi.org/10.1016/j.jhydrol.2022.127764

Duan, Q., Sorooshian, S., & Gupta, V. K. (1994). Optimal use of the SCE-UA global optimization method for calibrating watershed models. *Journal of Hydrology, 158*(3), 265-284. doi:https://doi.org/10.1016/0022-1694(94)90057-

4

Flinchum, B. A., Holbrook, W. S., Grana, D., Parsekian, A. D., Carr, B. J., Hayes, J. L., & Jiao, J. (2018). Estimating the water holding capacity of the critical zone using near-surface geophysics. *Hydrological Processes, 32*(22), 3308-3326. doi:https://doi.org/10.1002/hyp.13260

Fraga, I., Cea, L., & Puertas, J. (2019). Effect of rainfall uncertainty on the performance of physically based rainfall–runoff models. *Hydrological Processes, 33*(1), 160-173. doi:https://doi.org/10.1002/hyp.13319

Gentilucci, M., Barbieri, M., & Pambianchi, G. (2022). Reliability of the IMERG product through reference rain gauges in Central Italy. *Atmospheric Research, 278*, 106340. doi:https://doi.org/10.1016/j.atmosres.2022.106340

Ghimire, G. R., Krajewski, W. F., Ayalew, T. B., & Goska, R. (2022). Hydrologic investigations of radar-rainfall error propagation to rainfall-runoff model hydrographs. *Advances in Water Resources, 161*, 104145. doi:https://doi.org/10.1016/j.advwatres.2022.104145

Goshime, D. W., Absi, R., & Ledésert, B. (2019). Evaluation and bias correction of CHIRP rainfall estimate for rainfall-runoff simulation over Lake Ziway watershed, Ethiopia. *Hydrology, 6*(3), 68.

Gupta, L., & Dixit, J. (2022). Estimation of rainfall-induced surface runoff for the Assam region, India, using the GIS-based NRCS-CN method. *Journal of Maps, 18*(2), 428-440. doi:10.1080/17445647.2022.2076624

Hjelmstad, A., Shrestha, A., Garcia, M., & Mascaro, G. (2021). Propagation of radar rainfall uncertainties into urban pluvial flood modeling during the North American monsoon. *Hydrological sciences journal, 66*(15), 2232-2248. doi:10.1080/02626667.2021.1980216

Hsueh, H.-F., Guthke, A., Wöhling, T., & Nowak, W. (2022). Diagnosis of Model Errors With a Sliding Time-Window Bayesian Analysis. *Water Resources Research, 58*(2), e2021WR030590. doi:https://doi.org/10.1029/2021WR030590

Hussain, I., Spöck, G., Pilz, J., & Yu, H.-L. (2010). Spatio-temporal interpolation of precipitation during monsoon periods in Pakistan. *Advances in Water Resources, 33*(8), 880-886. doi:https://doi.org/10.1016/j.advwatres.2010.04.018

Hwang, S. H., Kim, K. B., & Han, D. (2020). Comparison of methods to estimate areal means of short duration rainfalls in small catchments, using rain gauge and radar data. *Journal of Hydrology, 588*, 125084. doi:https://doi.org/10.1016/j.jhydrol.2020.125084

Jie, M. X., Chen, H., Xu, C. Y., Zeng, Q., Chen, J., Kim, J. S., Guo, F. Q. (2018). Transferability of Conceptual Hydrological Models Across Temporal Resolutions: Approach and Application. *Water Resources Management, 32*(4), 1367-1381. doi:10.1007/s11269-017-1874-4

Kabir, T., Pokhrel, Y., & Felfelani, F. (2022). On the Precipitation-Induced

Uncertainties in Process-Based Hydrological Modeling in the Mekong River Basin. *Water Resources Research, 58*(2), e2021WR030828. doi:https://doi.org/10.1029/2021WR030828

Kim, C., & Kim, D.-H. (2020). Effects of Rainfall Spatial Distribution on the Relationship between Rainfall Spatiotemporal Resolution and Runoff Prediction Accuracy. *Water, 12*(3). doi:10.3390/w12030846

Li, J., Chen, H., Xu, C.-Y., Li, L., Zhao, H., Huo, R., & Chen, J. (2022). Joint Effects of the DEM Resolution and the Computational Cell Size on the Routing Methods in Hydrological Modelling. *Water, 14*(5). doi:10.3390/w14050797

Li, L., & Xu, C.-Y. (2014). The comparison of sensitivity analysis of hydrological uncertainty estimates by GLUE and Bayesian method under the impact of precipitation errors. *Stochastic Environmental Research and Risk Assessment, 28*(3), 491-504. doi:10.1007/s00477-013-0767-1

Li, W., Gao, X., Hao, Z., & Sun, R. (2022). Using deep learning for precipitation forecasting based on spatio-temporal information: a case study. *Climate Dynamics, 58*(1), 443-457. doi:10.1007/s00382-021-05916-4

Lilhare, R., Pokorny, S., Déry, S. J., Stadnyk, T. A., & Koenig, K. A. (2020). Sensitivity analysis and uncertainty assessment in water budgets simulated by the variable infiltration capacity model for Canadian subarctic watersheds. *Hydrological Processes, 34*(9), 2057-2075. doi:https://doi.org/10.1002/hyp.13711

Liu, J., Xu, L., & Chen, N. (2022). A spatiotemporal deep learning model ST-LSTM-SA for hourly rainfall forecasting using radar echo images. *Journal of Hydrology, 609*, 127748. doi:https://doi.org/10.1016/j.jhydrol.2022.127748

McMillan, H., Jackson, B., Clark, M., Kavetski, D., & Woods, R. (2011). Rainfall uncertainty in hydrological modelling: An evaluation of multiplicative error models. *Journal of Hydrology, 400*(1), 83-94. doi:https://doi.org/10.1016/j.jhydrol.2011.01.026

Merz, R., Parajka, J., & Blöschl, G. (2009). Scale effects in conceptual hydrological modeling. *Water Resources Research, 45*(9). doi:https://doi.org/10.1029/2009WR007872

Michelon, A., Benoit, L., Beria, H., Ceperley, N., & Schaefli, B. (2021). Benefits from high-density rain gauge observations for hydrological response analysis in a small alpine catchment. *Hydrology and Earth System Sciences, 25*(4), 2301-2325. doi:10.5194/hess-25-2301-2021

Militino, A. F., Ugarte, M. D., Goicoa, T., & Genton, M. (2015). Interpolation of daily rainfall using spatiotemporal models and clustering. *International Journal of Climatology, 35*(7), 1453-1464. doi:https://doi.org/10.1002/joc.4068

Niu, G., Yang, P., Zheng, Y., Cai, X., & Qin, H. (2021). Automatic Quality Control of Crowdsourced Rainfall Data With Multiple Noises: A Machine

Learning Approach. *Water Resources Research, 57*(11), e2020WR029121. doi:https://doi.org/10.1029/2020WR029121

Pang, J., Zhang, H., Xu, Q., Wang, Y., Wang, Y., Zhang, O., & Hao, J. (2020). Hydrological evaluation of open-access precipitation data using SWAT at multiple temporal and spatial scales. *Hydrology and Earth System Sciences, 24*(7), 3603-3626. doi:10.5194/hess-24-3603-2020

Qi, W.-y., Chen, J., Li, L., Xu, C.-Y., Li, J., Xiang, Y., & Zhang, S. (2022). Regionalization of catchment hydrological model parameters for global water resources simulations. *Hydrology Research, 53*(3), 441-466. doi:10.2166/nh.2022.118

Qi, W.-y., Chen, J., Li, L., Xu, C.-Y., Xiang, Y.-h., Zhang, S.-b., & Wang, H.-M. (2021). Impact of the number of donor catchments and the efficiency threshold on regionalization performance of hydrological models. *Journal of Hydrology, 601*, 126680. doi:https://doi.org/10.1016/j.jhydrol.2021.126680

Qiu, Y., da Silva Rocha Paz, I., Chen, F., Versini, P. A., Schertzer, D., & Tchiguirinskaia, I. (2021). Space variability impacts on hydrological responses of nature-based solutions and the resulting uncertainty: a case study of Guyancourt (France). *Hydrology and Earth System Science, 25*(6), 3137-3162. doi:10.5194/hess-25-3137-2021

Saft, M., Western, A. W., Zhang, L., Peel, M. C., & Potter, N. J. (2015). The influence of multiyear drought on the annual rainfall-runoff relationship: An Australian perspective. *Water Resources Research, 51*(4), 2444-2463. doi:https://doi.org/10.1002/2014WR015348

Saha, A., Singh, K. N., Ray, M., & Rathod, S. (2020). A hybrid spatio-temporal modelling: an application to space-time rainfall forecasting. *Theoretical and Applied Climatology, 142*(3), 1271-1282. doi:10.1007/s00704-020-03374-2

Sapriza-Azuri, G., Jódar, J., Navarro, V., Slooten, L. J., Carrera, J., & Gupta, H. V. (2015). Impacts of rainfall spatial variability on hydrogeological response. *Water Resources Research, 51*(2), 1300-1314. doi:https://doi.org/10.1002/2014WR016168

Sheng, S., Chen, H., Guo, F.-Q., Chen, J., Xu, C.-Y., & Guo, S.-l. (2020). Transferability of a Conceptual Hydrological Model across Different Temporal Scales and Basin Sizes. Water Resources Management, 34(9), 2953-2968.

Sreeparvathy, V., & Srinivas, V. V. (2022). A Bayesian Fuzzy Clustering Approach for Design of Precipitation Gauge Network Using Merged Remote Sensing and Ground-Based Precipitation Products. *Water Resources Research, 58*(2), e2021WR030612. doi:https://doi.org/10.1029/2021WR030612

Tao, Z., Li, M., Si, B., & Pratt, D. (2021). Rainfall intensity affects runoff responses in a semi-arid catchment. *Hydrological Processes, 35*(4), e14100. doi:https://doi.org/10.1002/hyp.14100

Tirkey, A. S., Pandey, A. C., & Nathawat, M. S. (2014). Use of high-resolution satellite data, GIS and NRCS-CN technique for the estimation of rainfall-induced run-off in small catchment of Jharkhand India. *Geocarto International, 29*(7), 778-791. doi:10.1080/10106049.2013.841773

Tobler, W. (2004). On the First Law of Geography: A Reply. *Annals of the Association of American Geographers, 94*(2), 304-310. doi:10.1111/j.1467-8306.2004.09402009.x

Vargas, Z. C. M., Valdez, S. I., & Paredes-Tavares, J. (2021, 9-11 Aug. 2021). *Spatio-temporal interpolation of rainfall data in western Mexico.* Paper presented at the 2021 Mexican International Conference on Computer Science (ENC).

Verma, R., Sharif, M., & Husain, A. (2022). Application of HEC-HMS for Hydrological Modeling of Upper Sabarmati River Basin, Gujarat, India. *Modeling Earth Systems and Environment*. doi:10.1007/s40808-022-01411-9

Wan, Y., Chen, J., Xu, C.-Y., Xie, P., Qi, W., Li, D., & Zhang, S. (2021). Performance dependence of multi-model combination methods on hydrological model calibration strategy and ensemble size. *Journal of Hydrology, 603*, 127065. doi:https://doi.org/10.1016/j.jhydrol.2021.127065

Wang, J., Petersen, W. A., & Wolff, D. B. (2021). Validation of Satellite-Based Precipitation Products from TRMM to GPM. *Remote Sensing, 13*(9). doi:10.3390/rs13091745

Wehbe, Y., Temimi, M., & Adler, R. F. (2020). Enhancing Precipitation Estimates Through the Fusion of Weather Radar, Satellite Retrievals, and Surface Parameters. *Remote Sensing, 12*(8). doi:10.3390/rs12081342

Wu, H., Yang, Q., Liu, J., & Wang, G. (2020). A spatiotemporal deep fusion model for merging satellite and gauge precipitation in China. *Journal of Hydrology, 584*, 124664. doi:https://doi.org/10.1016/j.jhydrol.2020.124664

Xu, H., Xu, C.-Y., Chen, H., Zhang, Z., & Li, L. (2013). Assessing the influence of rain gauge density and distribution on hydrological model performance in a humid region of China. *Journal of Hydrology, 505*, 1-12. doi:https://doi.org/10.1016/j.jhydrol.2013.09.004

Xu, M., Yang, Y., Han, M., Qiu, T., & Lin, H. (2019). Spatio-Temporal Interpolated Echo State Network for Meteorological Series Prediction. *IEEE Transactions on Neural Networks, 30*(6), 1621-1634.

Yang, W., Chen, H., Xu, C.-Y., Huo, R., Chen, J., & Guo, S. (2020). Temporal and spatial transferabilities of hydrological models under different climates and underlying surface conditions. *Journal of Hydrology, 591*, 125276. doi:https://doi.org/10.1016/j.jhydrol.2020.125276

Yang, X., Magnusson, J., Huang, S., Beldring, S., & Xu, C.-Y. (2020). Dependence of regionalization methods on the complexity of hydrological models in multiple climatic regions. *Journal of Hydrology, 582*, 124357. doi:https://doi.org/10.1016/j.jhydrol.2019.124357

Zhao, R.-J. (1992). The Xinanjiang model applied in China. *Journal of*

Hydrology, 135(1-4), 371-381.

Zhao, Y., Nearing, M. A., & Guertin, D. P. (2022). Modeling hydrologic responses using multi-site and single-site rainfall generators in a semi-arid watershed. *International Soil and Water Conservation Research, 10*(2), 177-187. doi:https://doi.org/10.1016/j.iswcr.2021.09.003

TABLES

Table 1 Description of the parameters and its physical meaning of the Xinanjiang model.

Classification	Parameter	Physical meaning	Range
Evapotranspiration	KE	Ratio of potential evapotranspiration to pan evaporation	0.6-2
	X	the coefficient of the upper layer tension water storage capacity	0.1-1
	Y	the coefficient of the lower layer tension water storage capacity	0.1-1
	C	Evapotranspiration coefficient of deep layer	0.15-0.2
Runoff production	WM	Areal mean tension water storage capacity	100-150
	B	Exponent of the tension water-capacity distribution curve	0.1-0.8
	IMP	Factor of impervious area	0.01-0.4
Runoff separation	SM	Free water-storage capacity	10-80
	EX	Exponential of distribution of free water-storage capacity	1.0-1.5
	KI	Out flow coefficient of free water storage to interflow	0.01-0.45
	KG	Out flow coefficient of free water storage to groundwater flow	0.01-0.6
Flow routing	CI	Recession constant of lower-interflow storage	0.7-1
	CG	Recession constant of groundwater storage	0.97-1
	N	Parameter of Nash unit hydrograph	0.5-12
	NK	Parameter of Nash unit hydrograph	0.8-25

Table 2 Optimal parameters sets obtained by SCE-UA algorithm.

parameter	WYS	MS	JY	SJ	SX	XC	QLJ
WM	123.90	143.56	104.27	115.79	142.82	132.46	137.39
X	0.10	0.09	0.16	0.17	0.09	0.10	0.14
Y	0.66	0.62	0.94	0.69	0.52	0.60	0.58
KE	0.93	1.85	1.87	1.16	1.65	1.96	1.65
B	0.42	0.39	0.45	0.40	0.40	0.40	0.44
SM	32.92	28.94	28.77	38.27	25.59	45.34	47.38
EX	1.11	1.41	1.07	1.47	1.37	1.37	1.10
KG	0.54	0.45	0.42	0.38	0.37	0.36	0.40
KI	0.26	0.34	0.33	0.40	0.37	0.36	0.33
IMP	0.25	0.13	0.22	0.25	0.22	0.30	0.30
C	0.17	0.16	0.15	0.18	0.17	0.18	0.19
CI	0.92	0.92	0.94	0.92	0.93	0.93	0.98
CG	0.99	0.99	0.99	0.99	0.97	0.98	0.99
N	1.15	3.08	4.28	2.18	1.51	2.92	4.74
NK	7.55	2.22	2.80	7.88	6.58	4.08	3.40

Table 3 Runoff simulation evaluation results of different areal rainfall based on the same set of parameters.

Sub-basin		WYS	MS	JY	SJ	SX	XC	QLJ	Average	Improvement rate (%)
Area(km2)		781	1072	4837	1653	3305	3060	14787		
NSE	AM	0.807	0.796	0.871	0.858	0.822	0.826	0.904	0.841	7.48 (10.24)
	TP	0.809(0.843)	0.809(0.831)	0.881(0.917)	0.865(0.891)	0.837(0.864)	0.864(0.860)	0.918(0.925)	0.855(0.876)	5.7 (5.78)
	F-SVD	0.860(0.886)	0.893(0.919)	0.926(0.955)	0.914(0.943)	0.872(0.899)	0.895(0.932)	0.964(0.953)	0.903(0.927)	-
RE	AM	0.09	0.183	0.117	0.046	0.117	0.108	0.064	0.103	58.8 (61.85)
	TP	0.035(0.033)	0.22(0.209)	0.079(0.075)	0.022(0.027)	0.109(0.103)	0.164(0.156)	0.058(0.055)	0.098(0.094)	56.5 (58.01)
	F-SVD	0.034(0.031)	0.091(0.084)	0.024(0.022)	0.05(0.046)	0.024(0.022)	0.033(0.031)	0.043(0.040)	0.042(0.039)	-
tAE(h)	AM	1.741	1.815	1.444	1.741	1.444	1.556	1.407	1.593	16.9 (24.19)
	TP	1.481(1.407)	1.556(1.478)	1.407(1.337)	1.63(1.549)	1.296(1.231)	1.481(1.407)	1.296(1.231)	1.45(1.377)	8.8 (12.32)
	F-SVD	1.481(1.352)	1.481(1.352)	1.185(1.082)	1.481(1.352)	1.259(1.149)	1.333(1.217)	1.037(0.947)	1.323(1.207)	-
vRE	AM	0.176	0.196	0.122	0.194	0.142	0.165	0.101	0.156	10.7 (18.91)
	TP	0.176(0.164)	0.199(0.185)	0.12(0.112)	0.179(0.166)	0.133(0.124)	0.168(0.156)	0.104(0.097)	0.153(0.143)	9.27 (11.44)
	F-SVD	0.177(0.160)	0.155(0.140)	0.105(0.095)	0.166(0.150)	0.129(0.117)	0.161(0.146)	0.089(0.081)	0.14(0.127)	-

† The number in the bracket is the runoff simulation results based on the parameters calibrated with areal rainfall using TP and F-SVD, respectively.

FIGURES

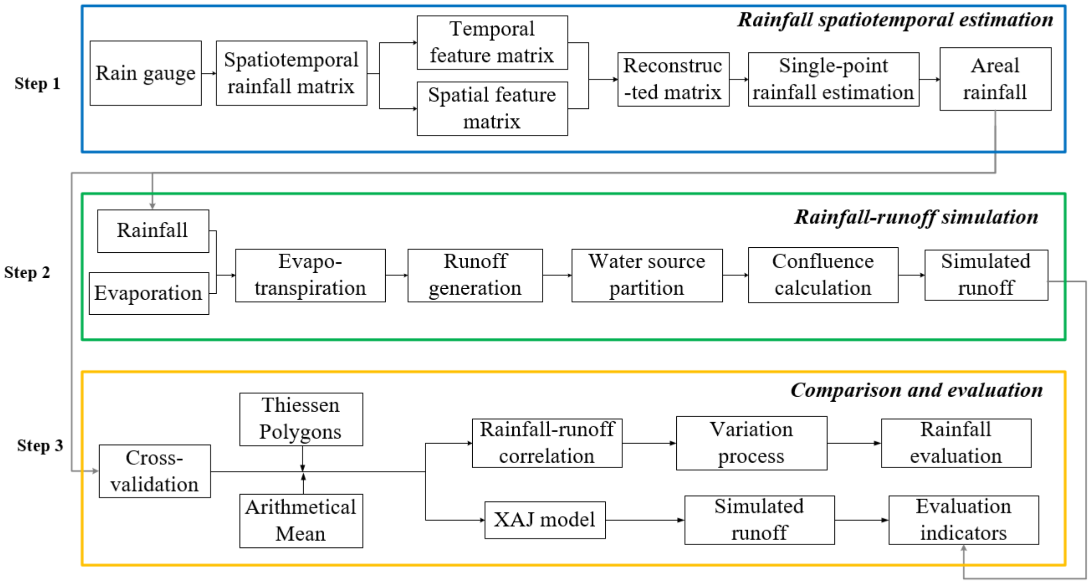

Figure 1. The flowchart of the research steps of this study.

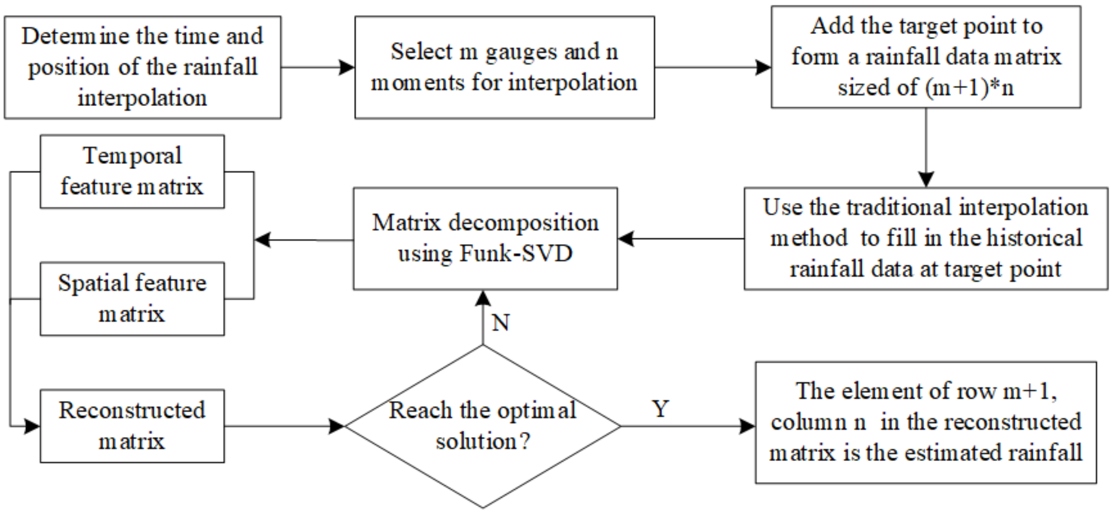

Figure 2. The calculation process of F-SVD.

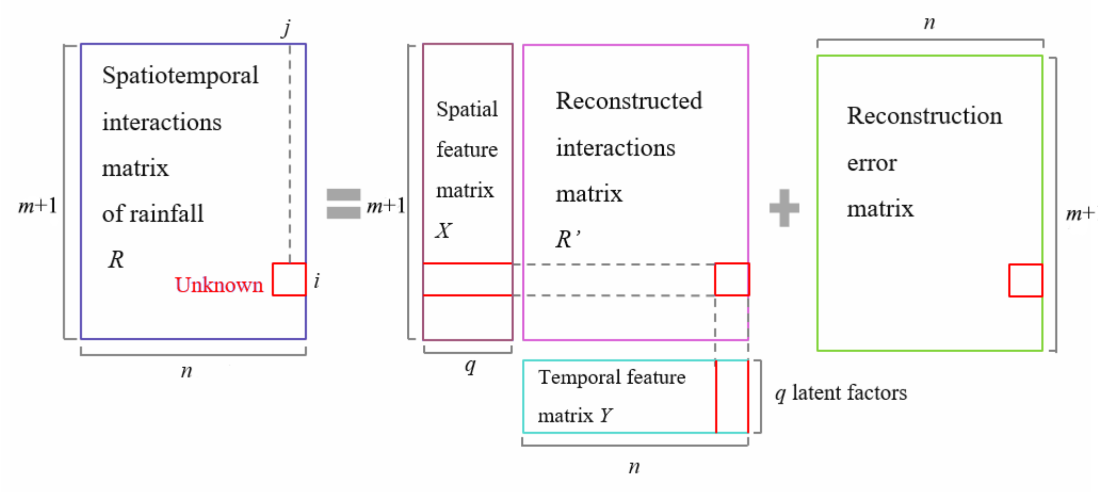

Figure 3. The proposed spatiotemporal estimation model based on F-SVD.

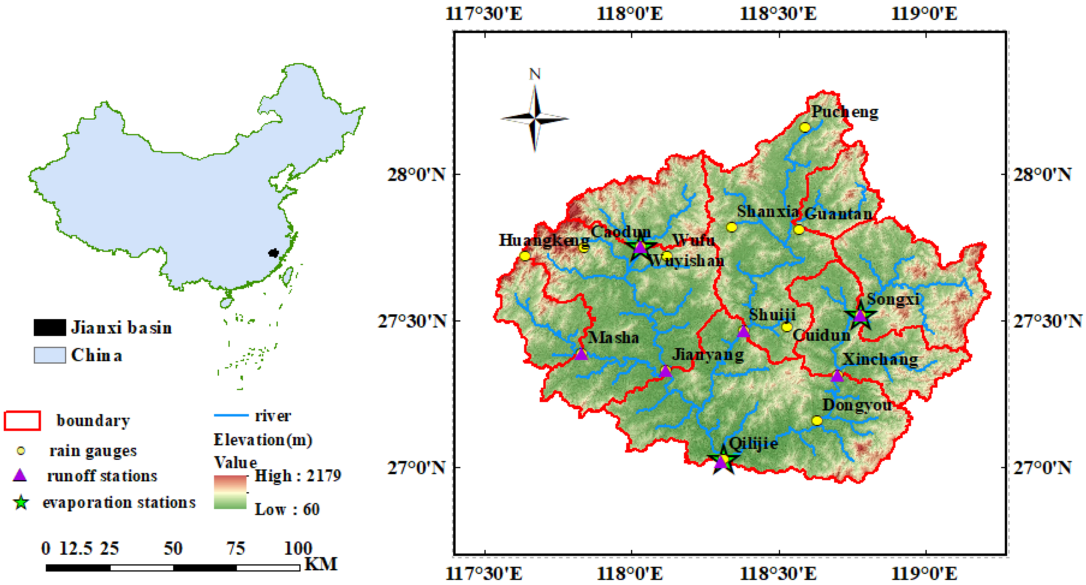

Figure 4. Geographical distribution of hydrological stations and sub-basins in Jianxi basin.

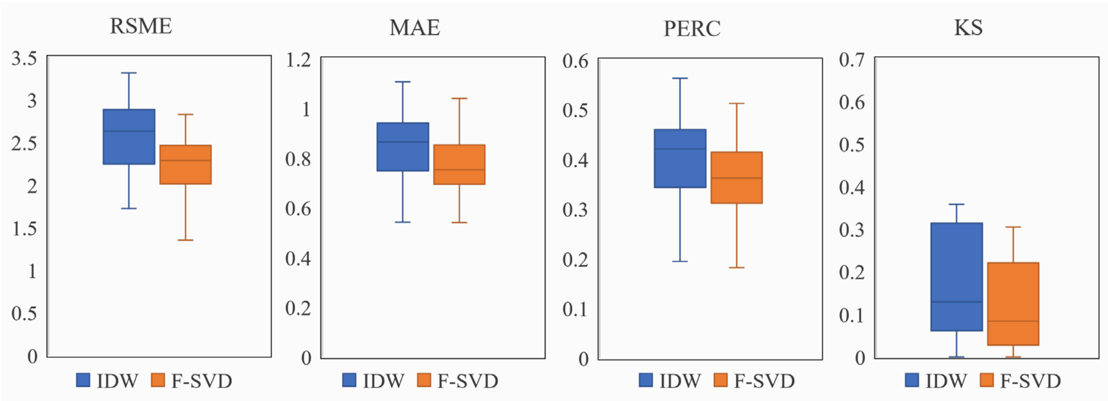

Figure 5. Boxplot of estimation accuracy of gauges in rainfall events.

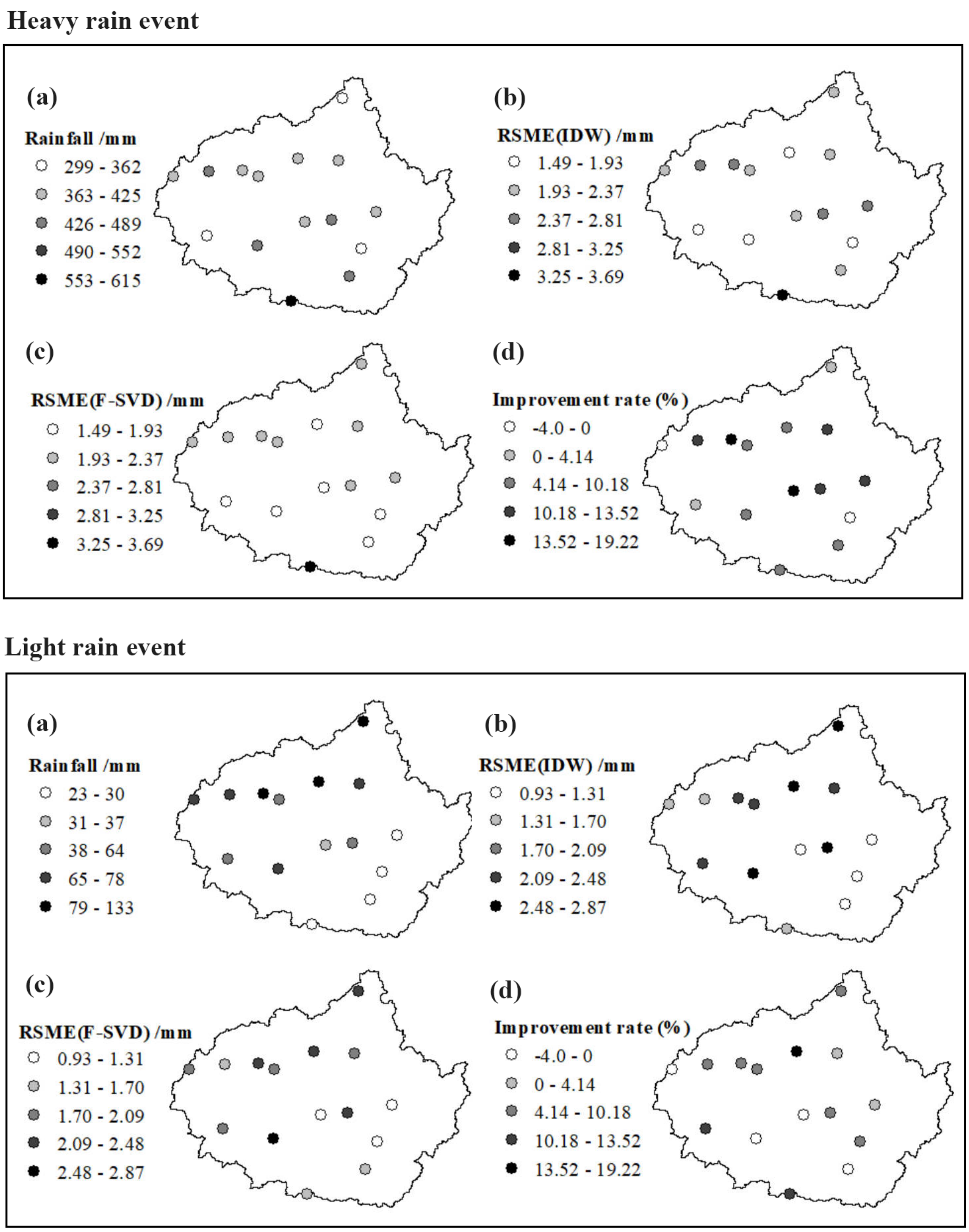

Figure 6. Comparison of the accuracy of F-SVD and IDW in cross-validation for heavy and light rain events. (**a**) Total observed rainfall of different gauges; (**b**) RSME of IDW in the cross-validation; (**c**) RSME of F-SVD in the cross-validation; (**d**) Accuracy improvement rate of F-SVD with respect to IDW.

Figure 7. Pearson correlation coefficients between three mean areal rainfall series and runoff observation series.

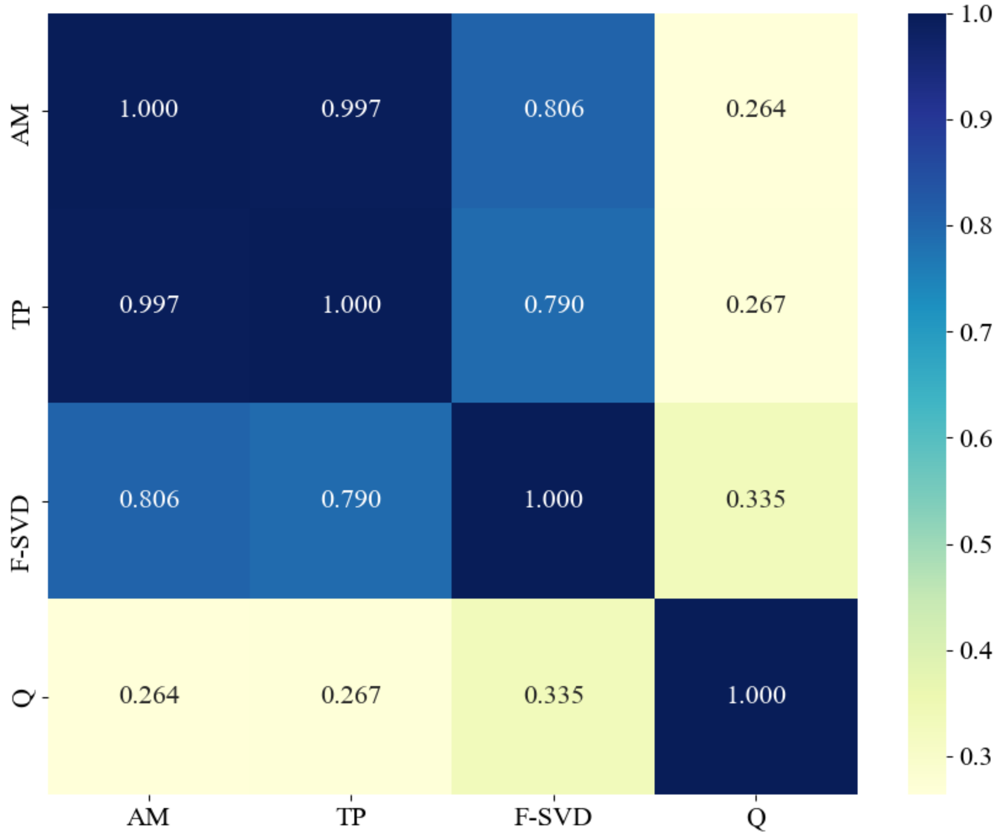

Figure 7. Pearson correlation coefficients between three mean areal rainfall series and runoff observation series.

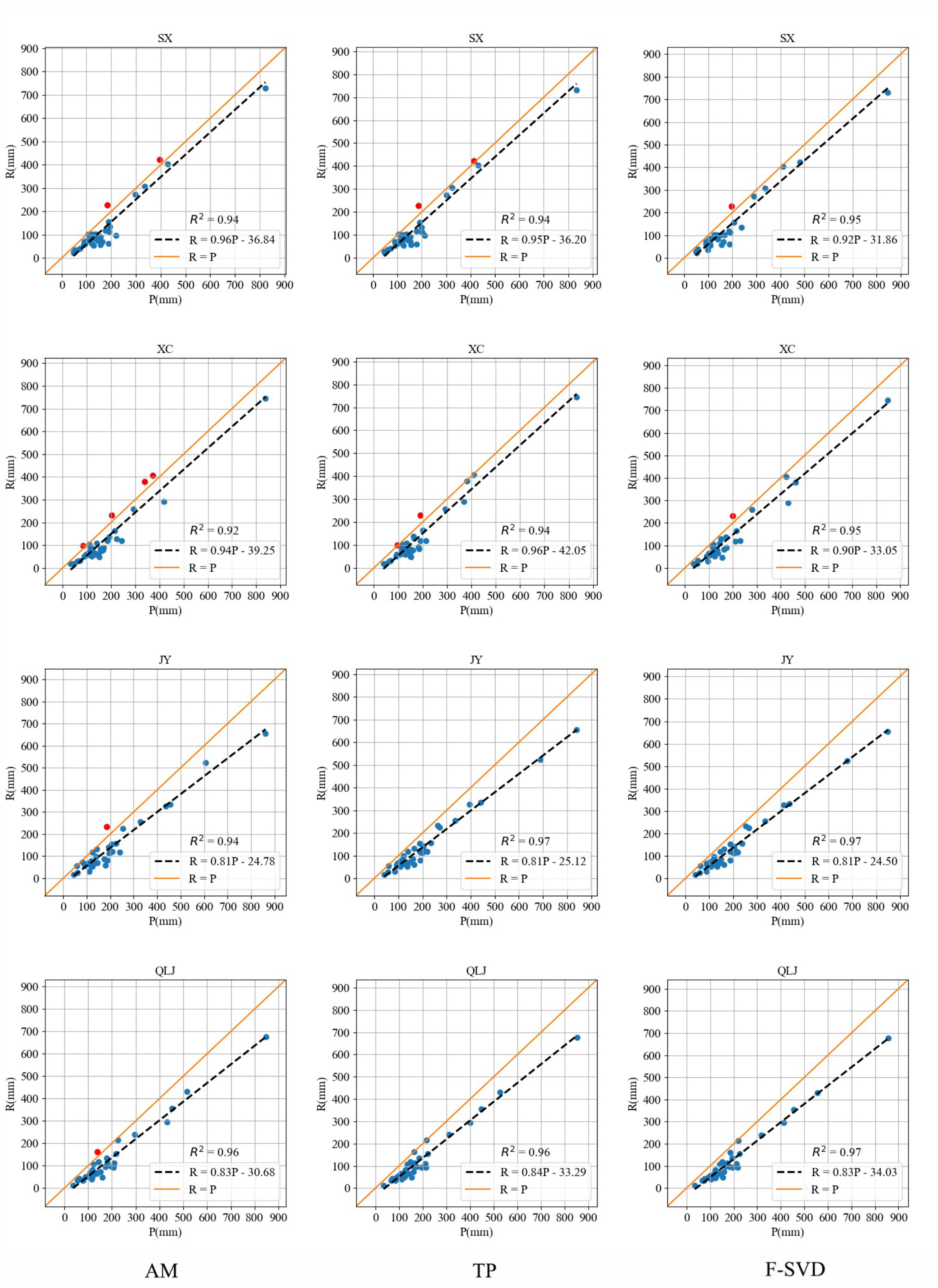

Figure 8. Correlation of rainfall and runoff of all floods. The blue dots indicate the floods with normal rainfall-runoff relationships, and the red dots indicate the abnormal floods when runoff depth exceeds total rainfall.

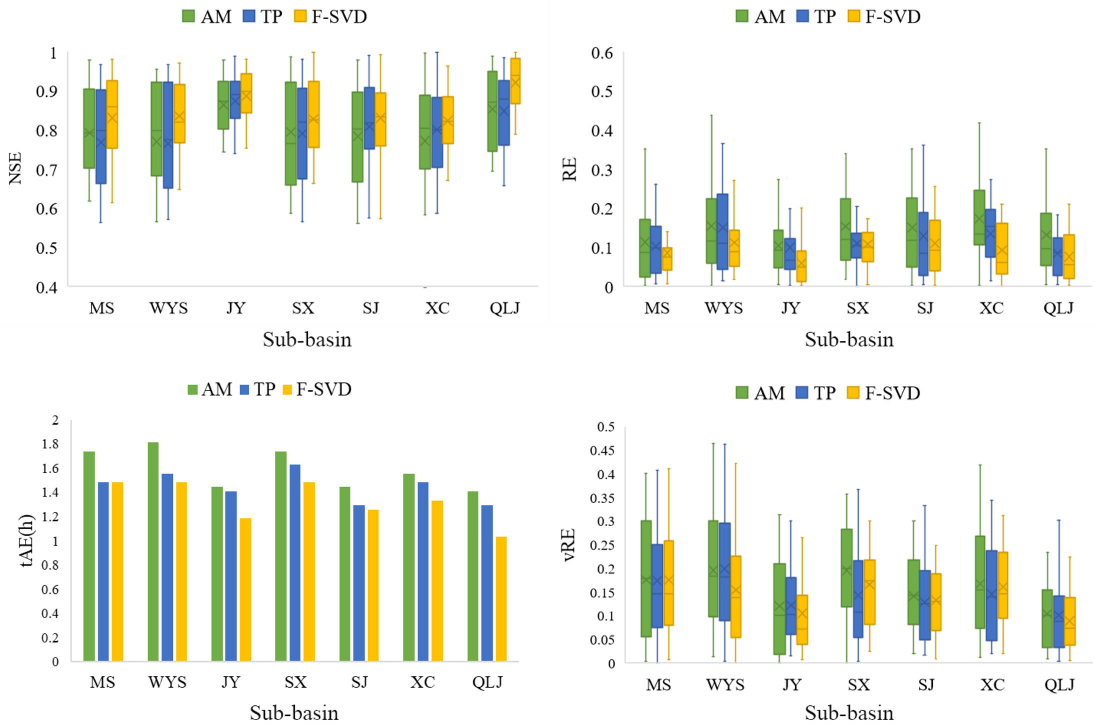

Figure 9. Accuracy of all flood simulations using different areal rainfall.

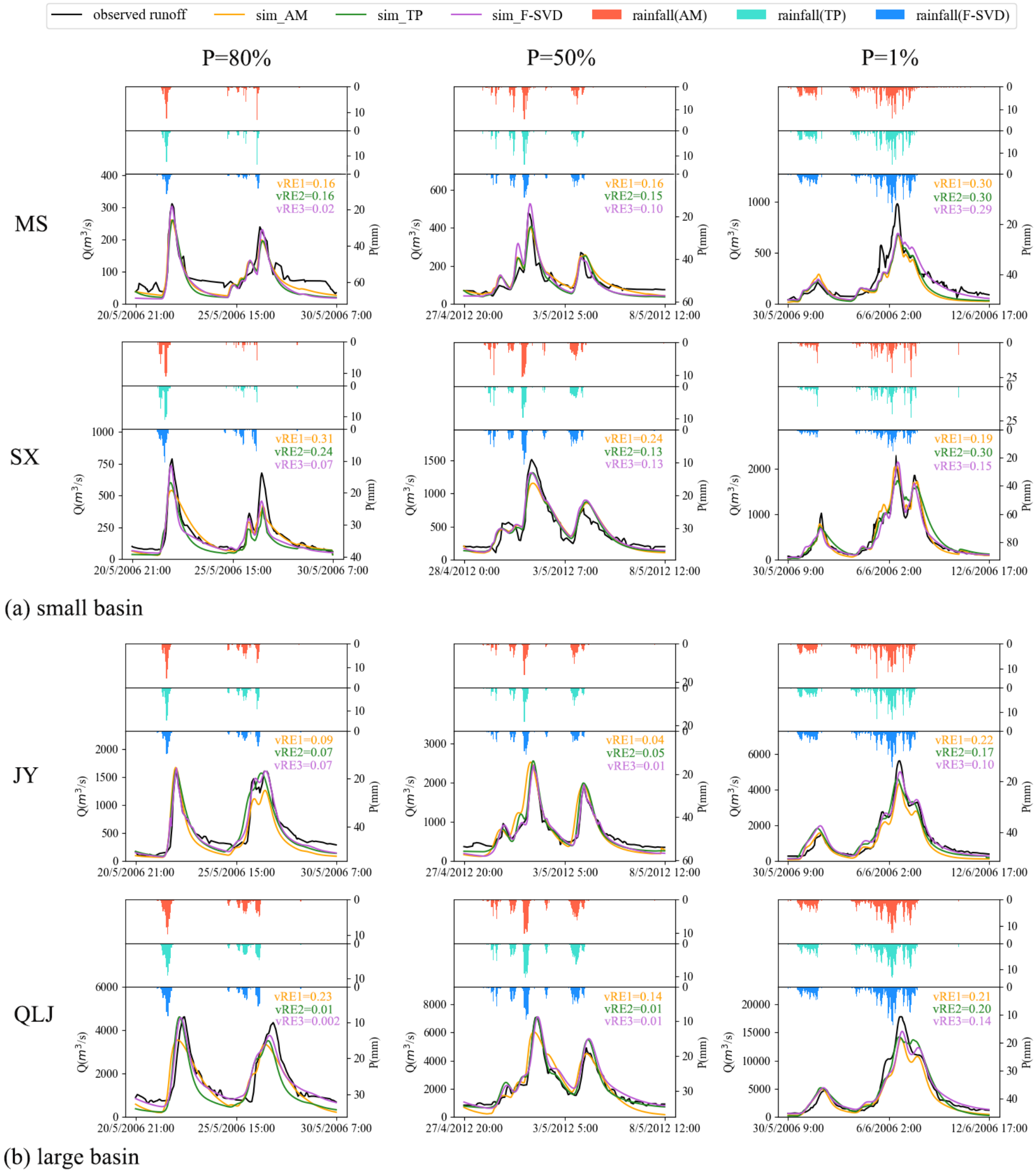

Figure 10. Simulated runoff processes for three typical flood events. *vRE*1, *vRE*2, and *vRE*3 refer to the *vRE* of simulated runoff based on the areal rainfall calculated by AM, TP, and F-SVD, respectively.